Mathematical Fluid Dynamics – Summer School, August 13-21 2021

Numerical computation of Navier-Stokes two-phase flows

Recent advances for strong stresses and open boundary conditions

Philippe Angot

Aix-Marseille Université
Institut de Mathématiques de Marseille
philippe.angot@univ-amu.fr

Institut d'Etudes Scientifiques de Cargèse (Corsica) – August 19, 2021

Target calculations in geophysical fluid dynamics

Surface water breaking waves : air/water coastal flow

Mythic Surf spot in Atlantic ocean at Belhara (Pays Basque, France)

Target calculations in geophysical fluid dynamics

Kelvin-Helmholtz instability :
one stratified fluid-phase or two-phase (liquid/gas) gravity waves

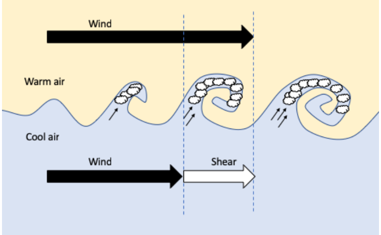

Kelvin-Helmholtz clouds in atmosphere

How to construct an efficient numerical method ?

Essential features for numerical solutions of multiphase flows :

- Variable density Navier-Stokes incompressible or low Mach number flows
- Two-phase flows with large density/viscosity ratios : $\boldsymbol{\rho_w/\rho_a \approx 10^3}$
- Moving interface $\boldsymbol{\Sigma}$ (between fluid immiscible phases) with large shape deformations
- Surface tension with possibly large capillarity coefficient on $\boldsymbol{\Sigma}$
- Coriolis rotation + suitable turbulence modelling
- Multi-physics coupling : temperature, salinity, Marangoni effect...

Reference books :

A. Prosperetti and G. Tryggvason (2007). Computational methods for multiphase flow

G. Tryggvason, R. Scardovelli, and S. Zaleski (2011). Direct numerical simulations of Gas-Liquid multiphase flows

How to construct an efficient numerical method ?

Main ingredients of a numerical solver in a bounded domain Ω with $\Gamma := \partial\Omega = \Gamma_D \cup \Gamma_N$ $(\Gamma_D \cap \Gamma_N = \emptyset)$:

1. Efficient velocity-pressure coupling with divergence-free constraint ?
   - for large density/viscosity ratios
   - for Dirichlet boundary condition on velocity : $\boldsymbol{v} = \boldsymbol{v_D}$ on $\boldsymbol{\Gamma_D}$, e.g. $\boldsymbol{v_D} = \boldsymbol{0}$
   - for Neumann open boundary condition : given stress vector $\boldsymbol{\sigma}(\boldsymbol{v}, \boldsymbol{p}) \cdot \boldsymbol{n} = \boldsymbol{g}$ on $\boldsymbol{\Gamma_N}$, e.g. $\boldsymbol{g} = -\boldsymbol{p_o}\,\boldsymbol{n}$

2. Accurate sharp ($\neq$ diffuse) interface capturing or front tracking methods ?
   - Volume of Fluid (VOF) methods : Hirt & Nichols (1981) – e.g. VOF-PLIC of Youngs (1982), Sarthou et al. (2008)
   - Level-set methods (LSM) : Thomasset & Dervieux (1979), Osher & Sethian (1988), Sethian (1999), Osher & Fedkiw (2002)
   - Immersed Interface Methods : Leveque & Li (1994), Li & Ito (2006), PhA. & Li (2017), Sarthou et al. (2020)
   - Arbitrary Lagrangian-Eulerian (ALE) methods
   - Lagrangian front tracking with advected interface markers : Hua & Tryggvason (2013) – Angot et al. (2016)
   - Phase-field methods (diffuse interface), e.g. with Cahn-Hilliard

Outlines

Objectives : efficient velocity-pressure coupling ?

Focus on the constraint of free velocity divergence $\operatorname{div} v = 0$

- Fully-coupled solver : ill-conditioned matrix of indefinite type
  $\Rightarrow$ Need efficient local preconditioners that are specific to the space discretization elements (FV, FE, DG,...)

- How to efficiently deal with the free-divergence constraint with splitting methods (prediction-correction steps) ?

- How to overcome most drawbacks of
  - Uzawa-augmented Lagrangian iterative methods
    Hestenes (1969) – Powell (1969) – Fortin & Glowinski (1983) ...
    Khadra et al., Int. J. Numer. Meth. Fluids (2000) (for MAC mesh)
  - scalar incremental projection or pressure correction methods
    Chorin (1968) – Temam (1969) – Goda (1979) – Van Kan (1986) ...
    Review : Guermond, Minev, Shen, CMAME (2006)

- Some improvements with the scalar penalty-projection method
  - Open Neumann stress B.C. : Jobelin et al., J. Comput. Phys. (2006) – PhA. et al., Int. J. Finite Volumes (2009)
  - Variable-density flow : Jobelin et al., Comput. Mech. (2008)

The orthogonal H.H. decomposition of $L^2(\Omega)^d$

Basics of pressure correction methods, e.g. Temam's book 1986 in a bounded open set Ω of $\mathbb{R}^d$

$\mathbf{L^2}(\Omega)^d = \mathbf{H} \oplus G$ with

$$\mathbf{H} = \{u \in L^2(\Omega)^d;\ \operatorname{div} u = 0,\ u\cdot n_{|\Gamma} = 0 \text{ on } \Gamma\}$$

$$G = \mathbf{H}^\perp = \{u \in L^2(\Omega)^d;\ u = \nabla\phi,\ \phi \in H^1(\Omega)/\mathbb{R}\}$$

Hence, for all vector field $v \in L^2(\Omega)^d$, we have the unique decomposition :

$v = v_\psi + v_\phi$ with $v_\phi = \nabla\phi \in G$

and $v_\psi = \mathbf{rot}\,\psi \in \mathbf{H},\ \operatorname{div}\psi = 0$ if Ω simply connected

Standard solution for a scalar potential ϕ if $v \in \mathbf{H}_{div}(\Omega)$: Poisson problem with Neumann B.C.

$$\begin{cases} \Delta\phi = \operatorname{div} v & \text{in } \Omega \\ \nabla\phi\cdot n_{|\Gamma} = v\cdot n & \text{on } \Gamma, \quad \text{since } \displaystyle\int_\Omega \operatorname{div} v\, dx = \langle v\cdot n, 1\rangle_{-1/2,\Gamma} \end{cases}$$

Then : $v_\phi = \nabla\phi$ and $v_\psi = v - \nabla\phi$

The Navier-Stokes problem with given density

with Dirichlet or open (Neumann) B.C. and $\rho := \rho(x,t)$ given

$\Omega \subset \mathbb{R}^d$ $(d \leq 3)$, bounded and connected Lipschitz domain with the Lipschitz continuous boundary $\Gamma = \partial\Omega = \Gamma_D \cup \Gamma_N$ and $\Gamma_D \cap \Gamma_N = \emptyset$

$$\begin{cases} \rho\,(\partial_t v + (v\cdot\nabla)v) - \mu\,\Delta v + \nabla p = f & \text{in } \Omega \times (0,T) \\ \operatorname{div} v = 0 & \text{in } \Omega \times (0,T) \\ v = v_D & \text{on } \Gamma_D \times (0,T) \\ -p\,n + \mu\,\nabla v\cdot n = g & \text{on } \Gamma_N \times (0,T) \\ v(t=0) = v_0 & \text{in } \Omega \end{cases}$$

Neumann B.C., *i.e.* pseudo-stress or full stress vector given :

$$\sigma(v,p)\cdot n := -p\,n + 2\mu\,d(v)\cdot n = g \quad \text{on } \Gamma_N \times (0,T)$$

where $d(v) := \dfrac{1}{2}\left(\nabla v + (\nabla v)^T\right)$ symmetric part of velocity gradient

The scalar incremental projection (SIP) method

with Dirichlet or open (Neumann) B.C. and $\rho := \rho(x,t)$ given
e.g. first-order time accuracy (Euler), extension to 2nd-order...
Originally introduced for $\boldsymbol{\rho = cst}$ and $\boldsymbol{v = 0}$ on $\boldsymbol{\Gamma}$ and *ad-hoc* extended...

$$
(1)\ \begin{cases}
\rho^{n+1}\left(\dfrac{\widetilde{v}^{n+1} - v^n}{\delta t} + (v^n \cdot \nabla)\widetilde{v}^{n+1}\right) - \mu\,\Delta\widetilde{v}^{n+1} + \nabla p^n = f^{n+1} \\
\widetilde{v}^{n+1}_{|\Gamma_D} = v_D \\
(-p^n\, n + \mu\,\nabla\widetilde{v}^{n+1} \cdot n)_{|\Gamma_N} = g
\end{cases}
$$

$$
(2)\ \begin{cases}
\rho^{n+1}\,\dfrac{v^{n+1} - \widetilde{v}^{n+1}}{\delta t} + \nabla\phi^{n+1} = 0, \quad \text{with}\ \ \phi^{n+1} = p^{n+1} - p^n \\
\operatorname{div} v^{n+1} = 0
\end{cases}
$$

$$
\Longrightarrow \quad (3)\ \begin{cases}
\operatorname{div}\left(\dfrac{\delta t}{\rho^{n+1}}\nabla\phi^{n+1}\right) = \operatorname{div}\widetilde{v}^{n+1} \\
\nabla\phi^{n+1} \cdot n_{|\Gamma_D} = 0 \\
\phi^{n+1}_{|\Gamma_N} = 0
\end{cases}
$$

Motivation : overcome most drawbacks of SIP

Main drawbacks of any projection method including a scalar pressure correction step with a Poisson-like equation

- spurious pressure boundary layer in space with velocity Dirichlet B.C. due to the artificial B.C. introduced on pressure inherently !
- non optimal pressure error estimate for 2nd-order time schemes : splitting errors : velocity $\mathcal{O}(\delta t^2)$ – pressure $\mathcal{O}(\delta t^{\frac{3}{2}})$
- poor accuracy for open (or outflow) boundary conditions : splitting errors : velocity $\mathcal{O}(\delta t)$ – pressure $\mathcal{O}(\delta t^{\frac{1}{2}})$ (standard SIP) or $\mathcal{O}(\delta t^{\frac{3}{2}})$ – $\mathcal{O}(\delta t)$ (rotational version)
- poor convergence and locking effect for large density, viscosity, permeability ratios...

Conjecture : mainly due to the inherent scalar formulation of the method and to the spatial derivative of mass density
$\Rightarrow$ It degrades the original vector formulation and produces a loss of consistency...
$\Rightarrow$ Design a fully vector-consistent splitting method for the velocity

Objective : efficient velocity-pressure coupling ?

Focus on the constraint of free velocity divergence $div\, v = 0$

⇒ Key idea : introduce a splitting penalty method for the velocity...
both prediction and correction steps now solved for the velocity vector
⇒ Fully vector consistent splitting method with velocity correction

⇒ New point of view :
Instead of determining the pressure field $\boldsymbol{p}$ (the Lagrange multiplier)
Calculate an accurate and curl-free approximation of $\boldsymbol{\nabla p}$
(the force inducing motion)

⇒ Primary unknowns are now $(\boldsymbol{v},\, \boldsymbol{\nabla p})$ instead of $(\boldsymbol{v},\, \boldsymbol{p})$

⇒ Counterpart : approximate divergence-free projection in the semi-discrete setting but the penalty parameter $\boldsymbol{\varepsilon}$ can be taken as small as desired.

Outlines

A new fast decomposition of $L^2(\Omega)^d$: DHHD I

PhA., Caltagirone and Fabrie, Appl. Math. Lett. (2013)

Key idea : design a suitable approximation by penalization of the curl-free component $\boldsymbol{v}_\phi = \boldsymbol{\nabla}\phi$ such that :

$$\operatorname{div} \boldsymbol{v}_\phi = \operatorname{div} \boldsymbol{v} \quad \text{and} \quad \mathbf{rot}\, \boldsymbol{v}_\phi = \mathbf{0} \ \text{ in } \ \boldsymbol{\Omega} \quad \text{with} \quad \boldsymbol{v}_\phi \cdot \boldsymbol{n}_{|\boldsymbol{\Gamma}} = \boldsymbol{v} \cdot \boldsymbol{n} \ \text{ on } \ \boldsymbol{\Gamma}$$

$\Rightarrow$ The so-called vector penalty-projection problem for all $\boldsymbol{\varepsilon} > \mathbf{0}$:

$$(\mathrm{VPP}_{\boldsymbol{n}}) \quad \begin{cases} \boldsymbol{\varepsilon}\, \boldsymbol{v}_\phi^\varepsilon - \boldsymbol{\nabla}\left(\operatorname{div} \boldsymbol{v}_\phi^\varepsilon\right) = -\boldsymbol{\nabla}\left(\operatorname{div} \boldsymbol{v}\right) \ \text{ in } \ \boldsymbol{\Omega} \\ \boldsymbol{v}_\phi^\varepsilon \cdot \boldsymbol{n}_{|\boldsymbol{\Gamma}} = \boldsymbol{v} \cdot \boldsymbol{n} \ \text{ on } \ \boldsymbol{\Gamma} \end{cases}$$

$$\Rightarrow \quad \begin{cases} \boldsymbol{v}_\phi^\varepsilon = \dfrac{\mathbf{1}}{\boldsymbol{\varepsilon}} \boldsymbol{\nabla}\left(\operatorname{div}\left(\boldsymbol{v}_\phi^\varepsilon - \boldsymbol{v}\right)\right) := \boldsymbol{\nabla}\phi^\varepsilon, \quad \mathbf{rot}\, \boldsymbol{v}_\phi^\varepsilon = \mathbf{0} \\ \phi^\varepsilon = \dfrac{\mathbf{1}}{\boldsymbol{\varepsilon}} \operatorname{div}\left(\boldsymbol{v}_\phi^\varepsilon - \boldsymbol{v}\right) \end{cases}$$

N.B. Extra regularity : $(\boldsymbol{v}_\phi - \boldsymbol{v}_\phi^\varepsilon) \in \mathbf{H}_{\mathbf{0},\boldsymbol{div}}(\boldsymbol{\Omega}) \cap \mathbf{H}_{\boldsymbol{rot}}(\boldsymbol{\Omega}) \hookrightarrow \mathbf{H}^{\mathbf{1}}(\boldsymbol{\Omega})$

$\Rightarrow$ Very well-conditioned whatever the mesh step $\boldsymbol{h}$ for $\boldsymbol{\varepsilon}$ small enough : effective conditioning independent of both $\boldsymbol{\varepsilon}$ and $\boldsymbol{h}$ due to adapted right-hand side !

A new fast decomposition of $L^2(\Omega)^d$: DHHD I

Weak form of (VPP$_n$) with the adapted right-hand side

For any $\boldsymbol{v} \in \mathbf{H}_{\boldsymbol{div}}(\boldsymbol{\Omega})$, using a standard Green's formula (integration by part), $\boldsymbol{v}_\phi^\varepsilon \in \mathbf{H}_{\boldsymbol{div}}(\boldsymbol{\Omega})$ satisfies :

$$\varepsilon \int_\Omega \boldsymbol{v}_\phi^\varepsilon \cdot \boldsymbol{\varphi}\, \boldsymbol{dx} + \int_\Omega (\operatorname{div} \boldsymbol{v}_\phi^\varepsilon)\,(\operatorname{div} \boldsymbol{\varphi})\, \boldsymbol{dx} - \left\langle \operatorname{div}(\boldsymbol{v}_\phi^\varepsilon - \boldsymbol{v}), \boldsymbol{\varphi}\cdot \boldsymbol{n} \right\rangle_{-1/2,\Gamma} = \int_\Omega (\operatorname{div} \boldsymbol{v})\,(\operatorname{div} \boldsymbol{\varphi})\, \boldsymbol{dx},$$

for all $\boldsymbol{\varphi} \in \mathbf{H}_{\boldsymbol{div}}(\boldsymbol{\Omega})$

Notice *a posteriori* that (VPP$_{\boldsymbol{n}}$) implies that : $\operatorname{div}(\boldsymbol{v}_\phi^\varepsilon - \boldsymbol{v}) \in \boldsymbol{H}^1(\boldsymbol{\Omega})$

Then, the boundary term vanishes with :

1. Essential B.C. : $\boldsymbol{\varphi}\cdot \boldsymbol{n} = \mathbf{0}$ on $\boldsymbol{\Gamma}$, then $\boldsymbol{\varphi} \in \mathbf{H}_{\mathbf{0},\boldsymbol{div}}(\boldsymbol{\Omega})$
2. Natural B.C. : $\operatorname{div}(\boldsymbol{v}_\phi^\varepsilon - \boldsymbol{v}) = \mathbf{0}$ on $\boldsymbol{\Gamma}$, *i.e.* "do nothing" for Neumann stress B.C.

$\Rightarrow$ Apply Lax-Milgram theorem for the solvability analysis in $\mathbf{H}_{\boldsymbol{div}}(\boldsymbol{\Omega})$

$\Rightarrow$ Then (VPP$_{\boldsymbol{n}}$) supplies the extra regularity :

$\boldsymbol{v}_\phi^\varepsilon \in \mathbf{H}_{\mathbf{0},\boldsymbol{div}}(\boldsymbol{\Omega}) \cap \mathbf{H}_{\boldsymbol{rot}}(\boldsymbol{\Omega}) \hookrightarrow \mathbf{H}^1(\boldsymbol{\Omega})$

Optimal accuracy of fast DHHD methods

PhA., Caltagirone and Fabrie, Appl. Math. Lett. (2013)

Theorem (Analysis of the vector penalty-projection (VPP_n).)

For any $\boldsymbol{v} \in \mathbf{H}_{div}(\Omega)$ *and all* $\varepsilon > 0$, *there exists a unique solution* $\boldsymbol{v}_\phi^\varepsilon$ *in* $\boldsymbol{H}_{div}(\Omega)$ *to the vector penalty-projection* (VPP_n).

Moreover, $\boldsymbol{v}_\phi^\varepsilon$ *is curl-free :* $\mathbf{rot}\, \boldsymbol{v}_\phi^\varepsilon = \mathbf{0}$, $\boldsymbol{v}_\phi^\varepsilon = \nabla \phi^\varepsilon \in \boldsymbol{G}$ *and* $div\,(\boldsymbol{v}_\phi^\varepsilon - \boldsymbol{v}) \in \boldsymbol{H}^1(\Omega) \cap \boldsymbol{L}_0^2(\Omega)$ *for all* $\varepsilon > 0$. *Then, we can choose* $\phi^\varepsilon \in \boldsymbol{H}^1(\Omega) \cap \boldsymbol{L}_0^2(\Omega)$ *such that* $div\,(\boldsymbol{v}_\phi^\varepsilon - \boldsymbol{v}) = \varepsilon\, \phi^\varepsilon$.

Besides, we have the following error estimates for all $\varepsilon > 0$ *:*

$$\|\boldsymbol{v}_\phi - \boldsymbol{v}_\phi^\varepsilon\|_1 + \|\phi - \phi^\varepsilon\|_2 + \|div\,(\boldsymbol{v} - \boldsymbol{v}_\phi^\varepsilon)\|_1 \leq c(\Omega)\, \|\boldsymbol{v}\|_0\, \varepsilon$$

N.B. Extra regularity : $(\boldsymbol{v}_\phi - \boldsymbol{v}_\phi^\varepsilon) \in \mathbf{H}_{0,div}(\Omega) \cap \mathbf{H}_{rot}(\Omega) \hookrightarrow \mathbf{H}^1(\Omega)$

⇒ Approximate divergence-free projection

⇒ Optimal accuracy of (VPP_n) as $\mathcal{O}(\varepsilon)$ with ε as small as desired up to machine precision

Typically : $\varepsilon = 10^{-14}$ with double precision

Conservation properties on edge-based generalized MAC-type unstructured meshes

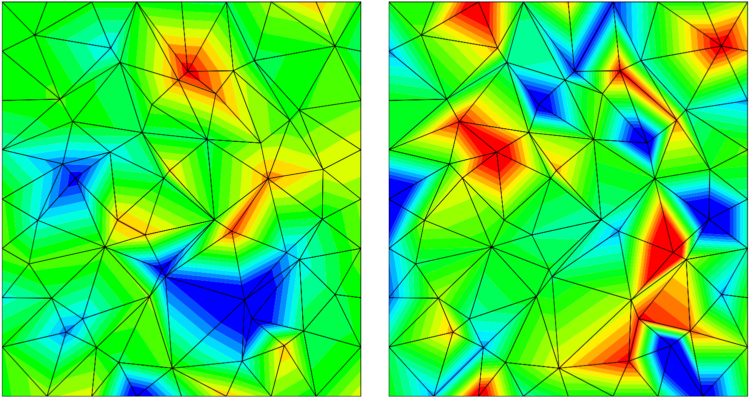

Discrete exterior calculus identities on a random Delaunay mesh for any typical analytic scalar field $\boldsymbol{\phi}$ or vector field $\boldsymbol{\psi}$.
LEFT : $\mathbf{rot}_h(\boldsymbol{\nabla}_h\boldsymbol{\phi}) = \pm\mathbf{1.7\,10^{-15}}$ in $\boldsymbol{\Omega}$
RIGHT : $\mathrm{div}_h(\mathbf{rot}_h\boldsymbol{\psi}) = \pm\mathbf{1.4\,10^{-14}}$ in $\boldsymbol{\Omega}$.

Solution cost of fast DHHD : (VPP) or (RPP)

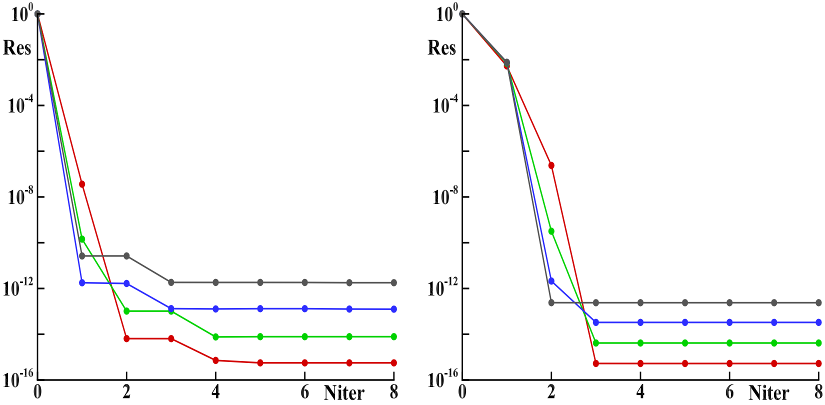

Convergence history of normalized residual of ILU(0)-BiCGstab2 solver for (RPP) or (VPP) problems with $\boldsymbol{\varepsilon = 10^{-14}}$ for different MAC mesh sizes $\mathbf{32 \times 32}$ (red), $\mathbf{128 \times 128}$ (green), $\mathbf{512 \times 512}$ (blue) and $\mathbf{2048 \times 2048}$ (black)

Left : Rotational Penalty-Projection (RPP)

Right : Vector Penalty-Projection (VPP)

$\Rightarrow$ Asymptotic optimal solver convergence within **2** or **3** iterations whatever $\boldsymbol{h}$ with $\boldsymbol{\varepsilon}$ as small as desired up to machine precision !

Solution cost of (VPP) step by PCG solvers

PhA. and Cheaytou, Commun. in Comput. Phys. (2019)

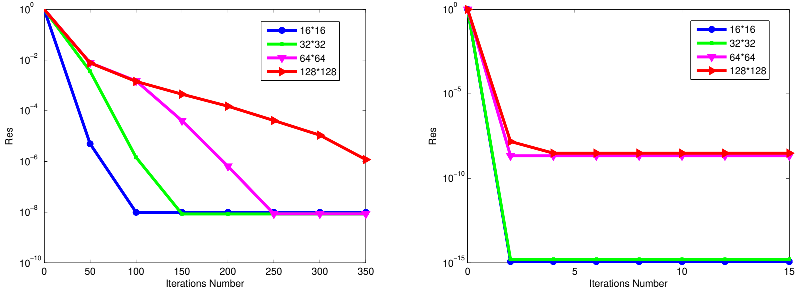

Convergence history of the normalized residual (by initial residual) of PCG solver for (VPP) problem at $\boldsymbol{T = 2\delta t}$ with $\boldsymbol{\delta t = 1}$ and $\boldsymbol{\varepsilon = 10^{-10}}$ for different mesh sizes
Left : Standard Conjugate Gradient (no preconditioner)
Right : Incomplete Choleski Preconditioned CG : IC(0)-PCG

$\Rightarrow$ Asymptotic optimal solver convergence within **4** iterations of IC(0)-PCG when $\boldsymbol{\varepsilon}$ is small enough whatever the mesh size $\boldsymbol{h}$

A splitting method for saddle-point problems

Recall : convergence rate of conjugate gradient method

Solve with $I = Id$ matrix of order n,
$B = -Div_h$: $m \times n$ matrix with $rank(B) = m < n$,
$B^T = Grad_h$:

$$(\varepsilon I + B^T B)\widehat{v}_\varepsilon = -B^T B \widetilde{v}$$

$$\mathcal{A}_\varepsilon := \varepsilon I + B^T B \quad \text{system matrix}$$

We have :

$$\kappa := \mathrm{cond}_2(\mathcal{A}_\varepsilon) = \frac{\varepsilon + \lambda_{max}(B^T B)}{\varepsilon} = \mathcal{O}\left(\frac{1}{\varepsilon}\right)$$

Number of iterations of preconditioned conjugate gradient solver :

$$\mathcal{N}_{iter} \leq \mathcal{O}\left(\sqrt{\kappa}\right) \qquad \text{bound for the worst case...}$$

The splitting penalty method :

- the system matrix $\mathcal{A}_\varepsilon$ is ill-conditioned for $\varepsilon \ll 1$
- but the system itself can be extremely well-conditioned due to the adapted right-hand side !

P.D.E. with adapted r.h.s. : a simple example

The simplified invertible case (continuous setting) :

Let $\Omega \subset \mathbb{R}^d$ be a bounded open domain, $u \in H_0^1(\Omega)$ given and $\varepsilon > 0$

Let us consider the problem (toy model) : find $u_\varepsilon \in H_0^1(\Omega)$ such that :

$$\begin{cases} \varepsilon\, u_\varepsilon - \Delta u_\varepsilon = -\Delta u, & \text{in } \Omega \\ u_\varepsilon = 0, & \text{on } \Gamma := \partial\Omega \end{cases}$$

We have the weak form, for all $v \in H_0^1(\Omega)$:

$$\varepsilon \int_\Omega (u_\varepsilon - u)\, v\, dx + \int_\Omega \nabla(u_\varepsilon - u) \cdot \nabla v\, dx = -\varepsilon \int_\Omega u\, v\, dx$$

and thus taking $v = u_\varepsilon - u$, we easily get with Poincaré inequality :

$$\|u_\varepsilon - u\|_{1,\Omega} \leq c(\Omega)\ \|\nabla(u_\varepsilon - u)\|_{0,\Omega} \leq C(\Omega)\ \|u\|_{0,\Omega}\ \varepsilon.$$

N.B. Here $-\Delta$ with Dirichlet B.C. is an invertible operator

$\Rightarrow$ Hence we can take $\varepsilon = 0$ and the solution is then trivial $u_0 = u$!

P.D.E. with adapted r.h.s. : a simple example

The simplified invertible case (discrete setting) :
$\Rightarrow$ asymptotic expansion of the solution u_ε

Let $A := -\Delta_h$ be the $n \times n$ symmetric positive definite matrix of the discrete Laplacian operator with homogeneous Dirichlet B.C.

It amounts to solve the linear system with an adapted r.h.s. :

$$(\varepsilon I + A)\, u_\varepsilon = Au.$$

We have :

$$\mathcal{A}_\varepsilon := (\varepsilon I + A) = A\left(I + \varepsilon A^{-1}\right)$$

$$\kappa := \mathrm{cond}_2(\mathcal{A}_\varepsilon) = \frac{\varepsilon + \lambda_{max}(A)}{\varepsilon + \lambda_{min}(A)} \longrightarrow_{\varepsilon \to 0} \mathrm{cond}_2(A) = \mathcal{O}\left(\frac{1}{h^2}\right)$$

If $\varepsilon < 1/\|A^{-1}\|$, we get the asymptotic expansion with a Neumann geometric serie :

$$\left(I + \varepsilon A^{-1}\right)^{-1} = \sum_{k=0}^{\infty} (-1)^k \varepsilon^k A^{-k}$$

$$\Rightarrow \quad u_\varepsilon = \left(I + \varepsilon A^{-1}\right)^{-1} u = u - \varepsilon A^{-1} u + \varepsilon^2 A^{-2} u - \cdots$$

P.D.E. with adapted r.h.s. : a simple example

The simplified invertible case (discrete setting) :
$\Rightarrow$ asymptotic expansion of the solution u_ε

Thus, with an adapted r.h.s. and $\varepsilon \ll 1$:

$$(\varepsilon I + A)\, u_\varepsilon = Au \quad \Rightarrow \quad u_\varepsilon = u + \mathcal{O}(\varepsilon)$$

$\Rightarrow$ zero-order term independent on A and the mesh step h !

But recall with a non adapted r.h.s. (usual case) and $\varepsilon \ll 1$:

$$(\varepsilon I + A)\, u_\varepsilon = f \quad \Rightarrow \quad u_\varepsilon = A^{-1}\, u + \mathcal{O}(\varepsilon)$$

The nice and surprising result for saddle-point

Non-invertible case with $A := B^T B$ ($B := -div_h$) : sketch of proof for a splitted saddle-point system with an adapted r.h.s.

PhA., Caltagirone and Fabrie, Appl. Math. Lett. 1 (2012)

$$(\varepsilon I + B^T B)\,\widehat{v}_\varepsilon = -B^T B\,\widetilde{v}$$

$$\mathcal{A}_\varepsilon := \varepsilon I + B^T B \quad \text{system matrix}$$

A key formula : Woodbury's formula (1949), a generalization of Sherman-Morrison's formula :

$$\left(I + \frac{1}{\varepsilon} B^T B\right)^{-1} = I - B^T \left(\varepsilon I + B B^T\right)^{-1} B, \quad \varepsilon > 0$$

Theorem : for any $m \times n$ matrix B with rank(B^T) = rank$(B) = m$
$\Rightarrow$ $\mathbf{ker}(B^T) = \{0\}$
$\Rightarrow$ the Schur complement $S := BB^T$ (Lagrange multiplier operator) is non singular
and if $\varepsilon < 1/\|S^{-1}\|$, we can do the asymptotic expansion with Neumann geometric serie and after either SVD or QR factorization, we get :

$$\widehat{v}_\varepsilon = -I_0\,\widetilde{v} + \mathcal{O}(\varepsilon), \quad I_0 = \text{diagonal matrix with only 1 or 0 entries}$$

Outlines

1. *Velocity-pressure coupling with* $div\, v = 0$
2. *Theoretical foundations of* VPP_ε *methods*
3. ***The family of*** VPP_ε ***methods***
   - Approximate divergence-free splitting methods
   - The artificial compressibility method revisited
   - Convergence analysis of VPP_ε for Navier-Stokes
   - Fast VPP_ε for multiphase N.S. flows
   - Fast Kinematic-VPP_ε for multiphase N.S. flows
4. *Sharp test cases with* VPP_ε*/K-*VPP_ε *methods*
5. *Conclusion and perspectives*

First-order vector penalty-projection method

Fast and fully vector-consistent VPP_ε splitting method :
PhA., C. and F., FVCA6 (2011) – Appl. Math. Lett. 2 (2012)
PhA. & C., CiCP (2019) : 2nd-order with BDF2 for open B.C.

$$(1)\begin{cases} \dfrac{\widetilde{v}^{n+1}-\widetilde{v}^{n}}{\delta t} + (v^n\cdot\nabla)\widetilde{v}^{n+1} - \dfrac{1}{\mathrm{Re}}\Delta\widetilde{v}^{n+1} + \nabla p^n = f^{n+1} & \text{in } \Omega \\ \widetilde{v}^{n+1} = v_D^{n+1} & \text{on } \Gamma_D \\ \sigma(\widetilde{v}^{n+1},p^n)\cdot n := -p^n\, n + 2\mu\, d(\widetilde{v}^{n+1})\cdot n = g^{n+1} & \text{on } \Gamma_N \end{cases}$$

$$(2)\begin{cases} \varepsilon\,\dfrac{\widehat{v}^{n+1}-\widehat{v}^{n}}{\delta t} - \nabla\left(\mathrm{div}\,\widehat{v}^{n+1}\right) = \nabla\left(\mathrm{div}\,\widetilde{v}^{n+1}\right) & \text{in } \Omega \\ \widehat{v}^{n+1}\cdot n = 0 \quad \text{or enforce} \quad \widehat{v}^{n+1} = 0 & \text{on } \Gamma_D \\ \widehat{v}^{n+1}\cdot n = 0 & \text{on } \Gamma_N \\ \text{or}\ \ \mathrm{div}\,\widehat{v}^{n+1} = -\mathrm{div}\,\widetilde{v}^{n+1} \quad \text{i.e. "do nothing" : } (\mathrm{div}\, v^{n+1})_{|\Gamma_N} = 0 & \text{on } \Gamma_N \end{cases}$$

$$\begin{cases} v^{n+1} = \widetilde{v}^{n+1} + \widehat{v}^{n+1} \quad \text{and} \quad p^{n+1} = p^n - \dfrac{1}{\varepsilon}\mathrm{div}\, v^{n+1} & \text{in } \Omega \\ \text{Pressure gradient correction to avoid round-off errors for very small } \varepsilon & \\ \nabla p^{n+1} = \nabla p^n - \dfrac{\widehat{v}^{n+1}-\widehat{v}^{n}}{\delta t} & \text{in } \Omega \end{cases}$$

The fast vector penalty-projection method

The artificial compressibility method revisited within two steps

$$\begin{cases} \dfrac{\widetilde{\boldsymbol{v}}^{n+1} - \widetilde{\boldsymbol{v}}^{n}}{\delta t} + (\boldsymbol{v}^{n} \cdot \nabla)\widetilde{\boldsymbol{v}}^{n+1} - \dfrac{1}{\mathrm{Re}}\Delta \widetilde{\boldsymbol{v}}^{n+1} + \nabla p^{n} = \boldsymbol{f}^{n+1} \\[2ex] \dfrac{\widehat{\boldsymbol{v}}^{n+1} - \widehat{\boldsymbol{v}}^{n}}{\delta t} - \dfrac{1}{\varepsilon}\nabla\left(\operatorname{div}\widehat{\boldsymbol{v}}^{n+1}\right) = \dfrac{1}{\varepsilon}\nabla\left(\operatorname{div}\widetilde{\boldsymbol{v}}^{n+1}\right) \\[2ex] \boldsymbol{v}^{n+1} = \widetilde{\boldsymbol{v}}^{n+1} + \widehat{\boldsymbol{v}}^{n+1} \\[2ex] \nabla(p^{n+1} - p^{n}) = -\dfrac{\widehat{\boldsymbol{v}}^{n+1} - \widehat{\boldsymbol{v}}^{n}}{\delta t} = -\dfrac{1}{\varepsilon}\nabla\left(\operatorname{div}\boldsymbol{v}^{n+1}\right) \end{cases}$$

VPP_ε ⇔ a new two-step artificial compressibility method

$$\begin{cases} \dfrac{\boldsymbol{v}^{n+1} - \boldsymbol{v}^{n}}{\delta t} + (\boldsymbol{v}^{n} \cdot \nabla)\widetilde{\boldsymbol{v}}^{n+1} - \dfrac{1}{\mathrm{Re}}\Delta \widetilde{\boldsymbol{v}}^{n+1} + \nabla p^{n+1} = \boldsymbol{f}^{n+1} \\[2ex] (\varepsilon\,\delta t)\,\dfrac{p^{n+1} - p^{n}}{\delta t} + \operatorname{div}\boldsymbol{v}^{n+1} = 0 \end{cases}$$

⇒ Better convergence than the one-step artificial compressibility method of Chorin-Temam, see [PhA. and Fabrie, Disc. Cont. Dyn. Syst. (2012)]

Unconditional stability of the VPP$_\varepsilon$ method

PhA., Caltagirone and Fabrie, Hal manuscript (2015)

Theorem (Global solvability and stability of the VPP$_\varepsilon$ method.)

For any $\boldsymbol{f} \in \boldsymbol{L}^2(0,T;\boldsymbol{H}^{-1}(\Omega)^d)$, $\boldsymbol{v}^0 \in \boldsymbol{L}^2(\Omega)^d$ *and* $\boldsymbol{p}^0 \in \boldsymbol{L}_0^2(\Omega)$ *given, the VPP$_\varepsilon$ method is well-posed for all* $0 < \delta t \leq T$ *and* $\varepsilon > 0$, i.e. *for all* $n \in \mathbb{N}$ *such that* $(n+1)\,\delta t \leq T$, *there exists a unique solution* $(\widetilde{v}^{n+1}, v^{n+1}, p^{n+1}) \in \boldsymbol{H}_0^1(\Omega)^d \times \boldsymbol{H}_n^1(\Omega)^d \times \boldsymbol{L}_0^2(\Omega)$ *to the VPP$_\varepsilon$ scheme such that :*

$$\frac{v^{n+1} - v^n}{\delta t} + (v^n \cdot \nabla)\widetilde{v}^{n+1} - \frac{1}{Re}\Delta \widetilde{v}^{n+1} + \nabla p^{n+1} = f^{n+1} \qquad \text{in } \Omega$$

$$(\varepsilon\,\delta t)\,\frac{p^{n+1} - p^n}{\delta t} + div\, v^{n+1} = 0 \qquad \text{in } \Omega$$

which is the discrete problem effectively solved by the splitting scheme. Moreover, we have unconditional stability of the VPP$_\varepsilon$ method for both velocity and pressure in the natural norms $l^\infty(0,T;L^2(\Omega)^d) \cap l^2(0,T;H^1(\Omega)^d)$ *and* $l^2(0,T;L^2(\Omega))$, *respectively.*

$\Rightarrow$ with compactness arguments (Aubin-Lions-Simon), we have :
Convergence to N.S. weak solutions in 3-D when $\varepsilon = \delta t$ tends to 0

Optimal error estimates of the VPP$_\varepsilon$ method

Second-order time accuracy with BDF2 scheme and open B.C. : See [PhA. and Cheaytou, SINUM 2019 (submitted)]

Theorem (Error estimates of VPP$_\varepsilon$ for Stokes with open B.C.)

With suitable sufficient regularity of the continuous solution $(\boldsymbol{v}, \boldsymbol{p})$ *and well-prepared initial conditions, we have for all* $0 < \delta t \leq \max(1, T)$ *and* $0 \leq \varepsilon \leq \mathcal{O}(\delta t)$ *: for all* $n \in \mathbb{N}$ *such that* $(n+1)\delta t \leq T$,

$$(i) \qquad \|e^{n+1}\|_0^2 + \varepsilon\delta t\,\|\pi^{n+1}\|_0^2 + \sum_{k=0}^{n} \frac{\delta t}{Re}\|\nabla e^{k+1}\|_0^2 \leq C\left(\delta t^4 + \varepsilon\,\delta t\right)$$

$$(ii) \qquad \sum_{k=0}^{n} \delta t\,\|\pi^{k+1} - \frac{1}{|\Omega|}\int_\Omega \pi^{k+1}\,dx\|_0^2 \leq C\left(\delta t^4 + \varepsilon\,\delta t\right)$$

$$(iii) \qquad \sum_{k=0}^{n} \delta t\,\|div\,v^{k+1}\|_0^2 = \sum_{k=0}^{n} \delta t\,\|div\,e^{k+1}\|_0^2 \leq C\left(\delta t^3 + \varepsilon\right)\varepsilon\,\delta t^2.$$

$\Rightarrow$ Better splitting errors for Dirichlet B.C. in $\mathcal{O}(\varepsilon\,\delta t^3 + \varepsilon^2\,\delta t^{3/2})$ instead of $\mathcal{O}(\varepsilon\,\delta t)$, see [PhA. and Cheaytou, Math. Comp. (2018)]

$\Rightarrow$ Error bounds confirmed by numerical results

Numerical results with MAC Cartesian mesh

Green-Taylor vortices : Navier-Stokes with Dirichlet B.C.

Divergence (discrete $\boldsymbol{l^\infty(0,T;L^2(\Omega))}$ norm) versus penalty $\boldsymbol{\varepsilon}$

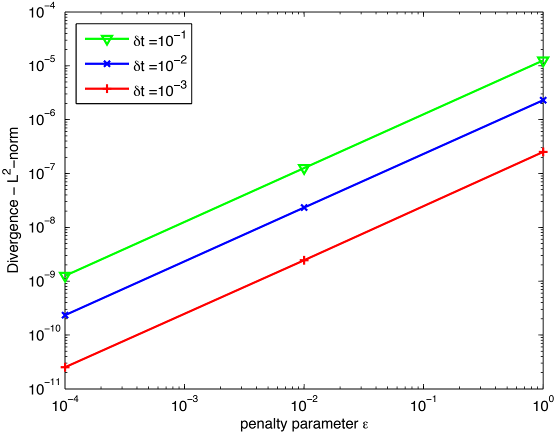

Divergence at Re $= \mathbf{100}$, $\boldsymbol{t = 10}$ - $\boldsymbol{h = 1/512}$, $\boldsymbol{|res|_2 < 10^{-10}}$

$\Rightarrow \|\mathrm{div}\, \boldsymbol{v^n}\|_{L^2} = \mathcal{O}(\varepsilon\, \delta t) = \mathcal{O}(\chi_{\mathcal{T}})$; velocity & pressure errors as $\mathcal{O}(\delta t^2)$

Numerical results with MAC Cartesian mesh

Stokes flow with homogeneous Neumann stress B.C.

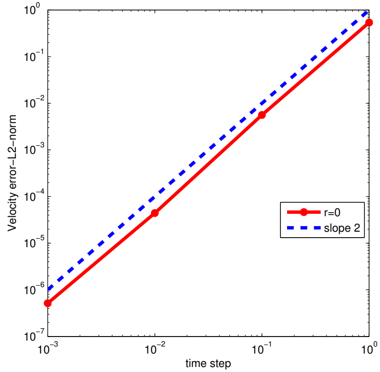

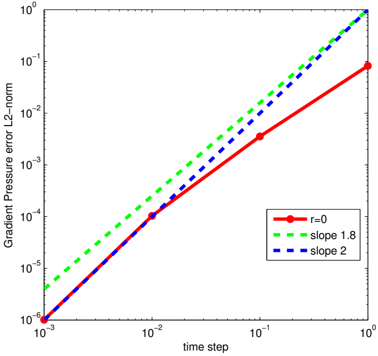

BDF2-VPP$_{\varepsilon}$ with OBC2 : time convergence rates at T=2, mesh size $h = 1/128$, $\varepsilon = 10^{-10}$ and $r = 0$

LEFT : velocity error L^2-norm

RIGHT : pressure gradient error L^2-norm

$\Rightarrow$ Optimal second-order accuracy : both velocity & pressure gradient errors as $\mathcal{O}(\delta t^2)$

A model for incompressible multiphase Navier-Stokes problems with capillary effects

$$\begin{cases} \rho(\varphi)\,(\partial_t\, v + (v\cdot\nabla)v) - 2\,\mathrm{div}\,(\mu\, d(v)) + \nabla p = f & \text{in } \Omega\times(0,T) \\ \mathrm{div}\, v = 0 & \text{in } \Omega\times(0,T) \\ \partial_t\,\varphi + v\cdot\nabla\varphi = 0 & \text{in } \Omega\times(0,T) \\ \text{or} \quad \partial_t\,\rho + v\cdot\nabla\rho = 0 & \text{in } \Omega\times(0,T) \end{cases}$$

with :

- the strain rate tensor : $d(v) := \frac{1}{2}\left(\nabla v + (\nabla v)^T\right)$
- f includes gravity force : $\rho\, g$ and surface tension on Σ : $\sigma\,\kappa\, n_\Sigma\,\delta_\Sigma$
  $\Leftrightarrow$ stress jump embedded conditions : $[\![\sigma(v,p)\cdot n]\!]_\Sigma = \sigma\,\kappa\, n_\Sigma$
- phase fraction (color) function : $\varphi \in [0,1]$ – at interface Σ :
  $\varphi = 0.5$ with VOF-PLIC method or use a level-set function $\varphi = 0$
- possibly coupled with the advection-diffusion equation for temperature $\mathcal{T}$ or salinity S
- given laws : $\rho = \rho(\mathcal{T}, S)$ and $\mu = \mu(\mathcal{T}, S)$ for each phase

A model for incompressible multiphase Navier-Stokes problems with capillary effects

The fast VPP_ε method, first-order linearly implicit scheme :

PhA., Caltagirone and Fabrie, 6th F.V.C.A. Conf. (2011) – Appl. Math. Lett. 2 (2012)

$$\rho^n \left(\frac{\widetilde{v}^{n+1} - v^n}{\delta t} + (v^n \cdot \nabla)\widetilde{v}^{n+1} \right) - 2\,\mathrm{div}\,\left(\mu^n\, d(\widetilde{v}^{n+1}) \right) + \nabla p^n = f^n$$

$$\frac{\varepsilon}{\delta t}\,\rho^n\,\widehat{v}^{n+1} - \nabla\left(\mathrm{div}\,\widehat{v}^{n+1}\right) = \nabla\left(\mathrm{div}\,\widetilde{v}^{n+1}\right)$$

$$v^{n+1} = \widetilde{v}^{n+1} + \widehat{v}^{n+1}$$

$\phi^{n+1} := p^{n+1} - p^n$ from $\nabla\phi^{n+1} := \nabla(p^{n+1} - p^n) = -\dfrac{\rho^n}{\delta t}\,\widehat{v}^{n+1}$

VOF-PLIC interface capturing : $\dfrac{\varphi^{n+1} - \varphi^n}{\delta t} + v^{n+1} \cdot \nabla\varphi^n = 0$

or by Lagrangian front tracking : $\dfrac{\rho^{n+1} - \rho^n}{\delta t} + v^{n+1} \cdot \nabla\rho^n = 0$

Kinematic version K-VPP$_\varepsilon$ for edge-based MAC

PhA., Caltagirone and Fabrie, C.R. Math. Acad. Sci. (2016)

$$\begin{cases} \rho^n \left(\dfrac{\widetilde{v}^{n+1} - v^n}{\delta t} + (v^n \cdot \nabla) \widetilde{v}^{n+1} \right) - \mathrm{div}\left(2\mu(\rho^n)\, d(\widetilde{v}^{n+1}) \right) + \nabla p^n = f^n & \text{in } \Omega \\ \widetilde{v}^{n+1}_{|\Gamma} = 0 & \text{on } \Gamma \\ \textbf{(b)} \text{ Divergence-free velocity penalty-projection (VPP) : purely kinematic step} & \\ \varepsilon\, \widehat{v}^{n+1} - \nabla \left(\mathrm{div}\, \widehat{v}^{n+1} \right) = \nabla \left(\mathrm{div}\, \widetilde{v}^{n+1} \right) & \text{in } \Omega \\ \widehat{v}^{n+1}_{|\Gamma} = 0 & \text{on } \Gamma \\ \textbf{(c)} \text{ Velocity correction : } \quad v^{n+1} = \widetilde{v}^{n+1} + \widehat{v}^{n+1} & \text{in } \Omega \\ \textbf{(d)} \text{ Find the inertial density } \overline{\rho}^n \text{ such that : } \nabla(\overline{\rho}^n\, \phi^{n+1}) = \rho^n\, \widehat{v}^{n+1} & \text{in } \Omega \\ \text{with } \phi^{n+1} \text{ reconstructed from its gradient } \widehat{v}^{n+1} := \nabla \phi^{n+1} & \\ \textbf{(e)} \text{ Explicit locally consistent pressure gradient correction : dynamic step} & \\ \nabla(p^{n+1} - p^n) = -\dfrac{\rho^n}{\delta t}\, \widehat{v}^{n+1} = -\dfrac{1}{\delta t} \nabla(\overline{\rho}^n\, \phi^{n+1}) & \text{in } \Omega \\ \textbf{(f)} \text{ Advection by Lagrangian front-tracking of density :} & \\ \dfrac{\rho^{n+1} - \rho^n}{\delta t} + v^{n+1} \cdot \nabla \rho^n = 0 & \text{in } \Omega \end{cases}$$

Edge-based generalized MAC unstructured mesh

A.C.F., Appl. Math. Lett. (2013) – C.R. Math. Acad. Sci. 2016

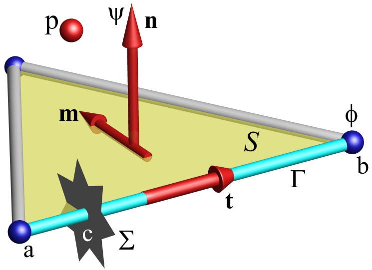

Topology of the 3-D primal mesh with vertices, edges, faces and an interface $\boldsymbol{\Sigma}$:
$\boldsymbol{p}, \boldsymbol{\rho}, \boldsymbol{\phi}$ unknowns located at all vertices $\boldsymbol{a}$ or $\boldsymbol{b}$ and velocity components $\boldsymbol{v} \cdot \boldsymbol{t}$ on each edge $[\boldsymbol{a}, \boldsymbol{b}]$

$\Rightarrow$ Important properties exactly satisfied in the discrete way :
$\mathbf{rot}_{\,h}(\boldsymbol{\nabla}_h \phi_h) = \mathbf{0}$ and $\mathrm{div}_{\,h}(\mathbf{rot}_{\,h} \psi_h) = \mathbf{0}$, $\forall h > 0$ for any scalar ϕ or vector potential ψ (up to machine precision)

$\Rightarrow$ Discrete compatibility condition satisfied $\boldsymbol{\nabla}_h(\overline{\rho}\,\phi) = \rho\,\widehat{v}$ with :
$\mathbf{rot}_{\,h}(\rho\,\widehat{v}) = \rho\,\mathbf{rot}_{\,h}\widehat{v} + \boldsymbol{\nabla}_h\rho \wedge \widehat{v} = \boldsymbol{\nabla}_h\rho \wedge \widehat{v} = \mathbf{0}$ since $\mathbf{rot}_{\,h}\widehat{v} = \mathbf{0}$

Reconstruction of potential ϕ such that : $\widehat{v} := \nabla\phi$

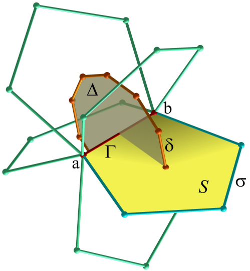

- Scalar potential ϕ reconstructed by integrating its known gradient $\widehat{v}$ along all the edges in the primal mesh
- Starting from one point where $\phi := 0$ arbitrarily, we have along any edge $[a, b]$:

$$\int_a^b \widehat{v} \cdot t \, dx := \int_a^b \nabla\phi \cdot t \, dx = \phi_b - \phi_a, \quad \text{on any edge } [a, b]$$

which gives the value ϕ_b when ϕ_a is already known and so on...

Calculation of density $\overline{\rho}$ such that : $\nabla(\overline{\rho}\,\phi) = \rho\,\widehat{v}$

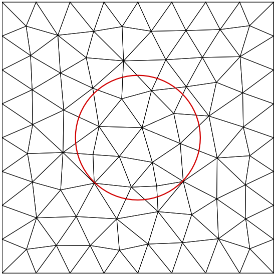

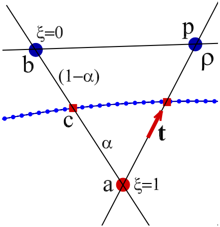

Primary mesh topology and interface $\boldsymbol{\Sigma}$ represented by a chain of connected Lagrangian markers

From one side using the generalized average formula, there exists $\overline{\boldsymbol{\rho}}$ constant along the segment $[\boldsymbol{a}, \boldsymbol{b}]$ such that :

$$\int_a^b \rho\,\widehat{v}\cdot t\,dx = \overline{\rho}\int_a^b \widehat{v}\cdot t\,dx = \overline{\rho}\,(\phi_b - \phi_a) = \int_a^b \nabla(\overline{\rho}\,\phi)\cdot t\,dx$$

$\Rightarrow \overline{\boldsymbol{\rho}}$ satisfies the compatibility condition : $\nabla(\overline{\rho}\,\phi) = \rho\,\widehat{v} = \rho\,\nabla\phi$ along the edge $[\boldsymbol{a}, \boldsymbol{b}]$

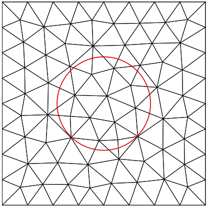

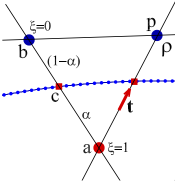

From another side, with $c := \Sigma \cap [a,b]$ and the distance $d(a,b) := |b-a|$:

$$\int_a^b \rho\,\widehat{v}\cdot t\,dx = \int_a^c \rho\,\widehat{v}\cdot t\,dx + \int_c^b \rho\,\widehat{v}\cdot t\,dx = (\rho_a\,|c-a| + \rho_b\,|b-c|)\,\widehat{v}\cdot t$$

$$= \frac{(\rho_a\,|c-a| + \rho_b\,|b-c|)}{|b-a|} \int_a^b \widehat{v}\cdot t\,dx$$

$$= (\alpha\,\rho_a + (1-\alpha)\,\rho_b)\;(\phi_b - \phi_a), \quad \text{with } \alpha := \frac{|c-a|}{|b-a|}.$$

Comparing the two expressions, we get $\overline{\rho}$ associated to the edge $[a,b]$ as a weighted average :

$$\overline{\rho}_{[a,b]} = \alpha\,\rho_a + (1-\alpha)\,\rho_b, \quad \text{on any intersected edge } [a,b], \quad 0 \le \alpha \le 1.$$

An accurate front-tracking Lagrangian advection

a) Calculate the barycentric velocity $\boldsymbol{v_b(x)}$ of each marker point $\boldsymbol{x}$ from the velocity components $\boldsymbol{v^{n+1}\cdot t}$ on the edges bordering the primal cell where the marker lies

b) Move the markers such that $\boldsymbol{x'(t) = v_b(t,x)}$ by calculating the new position with the Heun Runge-Kutta explicit scheme (RK2 or RK4 with the K-VPP method of second-order in time) :

$$\boldsymbol{x^{n+1} = x^n + \frac{\delta t}{2}\left(v_b^n(x^n) + v_b^{n+1}(x^n + \delta t\, v_b^n(x^n))\right)}.$$

c) Detect the cells in the primal mesh which are crossed by the updated marker chain with a ray-tracing technique issued from computer graphics procedures and according to that, update the phase function $\boldsymbol{\xi}$ at the vertices

d) Calculate the intersection points $\boldsymbol{x_\Sigma \in [a,b]}$ between the marker chain segments and the edges $\boldsymbol{[a,b]}$ of the crossed cells in the primal mesh

e) From $\boldsymbol{x_\Sigma}$, calculate the dividing function $\boldsymbol{\alpha}$ on each edge $\boldsymbol{[a,b]}$ oriented by $\boldsymbol{t}$ and cutted across by $\boldsymbol{\Sigma}$

f) Update the density $\boldsymbol{\rho(\xi)}$, the viscosity $\boldsymbol{\mu(\xi)}$ and the mass density $\boldsymbol{\overline{\rho}_{[a,b]} = \alpha\,\rho_a + (1-\alpha)\,\rho_b}$, on any intersected edge $\boldsymbol{[a,b]}$

g) Compute the local curvature $\boldsymbol{\kappa(x)}$ at each marker point $\boldsymbol{x}$ using the osculator circle crossing three consecutive points

h) Compute the force source term modelling the capillary effects $\boldsymbol{f_c := \sigma\,\kappa\,\nabla\xi}$ on $\boldsymbol{\Sigma}$ to be included in the force balance on any intersected edge

i) Solve for the flow at time $\boldsymbol{t^{n+1} = (n+1)\delta t}$ with the method of velocity-pressure coupling.

$\Rightarrow$ Good mass conservation of the different phases observed practically

Accurate calculation of the local curvature $\kappa(x)$

Local curvature $\kappa(x)$ calculated at each marker point x by using the osculator circle defined by x and its two neighbours in 2-D

- Exact when the interface Σ is a circle of radius R or a sphere in 3-D :
  $\kappa = 1/R$ (circle) or $\kappa = 2/R$ (sphere)
  $\Rightarrow$ Numerically verified up to machine precision
- For an ellipse of radius a and b in the polar coordinates :

$$\kappa(\theta) = \frac{a\,b}{(a^2\ \sin^2\theta + b^2\ \cos^2\theta)^{3/2}}, \quad \text{with}\ \ \theta \in [0, 2\pi].$$

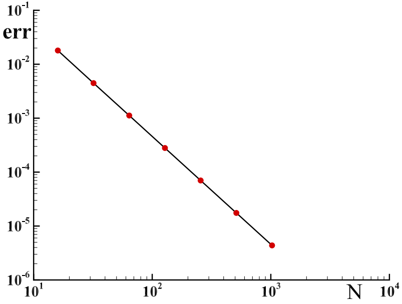

$\Rightarrow$ Second-order accuracy in the L^2-norm w.r.t. the mean distance between two connected interface-markers

Outlines

Sharp test case for fluid-structure interaction

ACF11-ball : free fall of an heavy rigid ball in air at time $t = 0.15$ and $Re = 7358$
VPP_ε method with $\varepsilon = 10^{-6}$, mesh size=256×512, $\delta t = 0.0002$

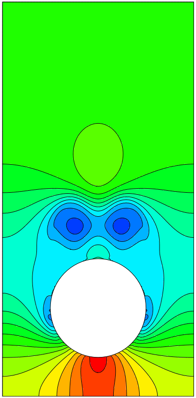

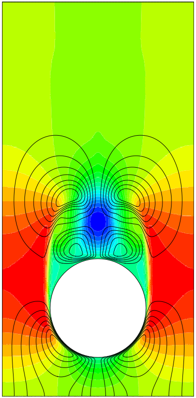

Cylinder diameter $d = 0.05$, $\rho_s = 10^6$, $\rho_f = 1$, $\mu_s = 10^{12}$, $\mu_f = 10^{-5}$, domain 0.1×0.2, cylinder initially with no motion at height $y = 0.15$.
LEFT : isobars and isoline $\varphi = 0.5$ of the phase function at interface.
RIGHT : vertical velocity field and horizontal velocity isolines.

Static equilibrium of a droplet : Laplace's law

First numerical method which eliminates the spurious eddies !

See e.g. book [Tryggvason, Scardovelli and Zaleski (2011)]

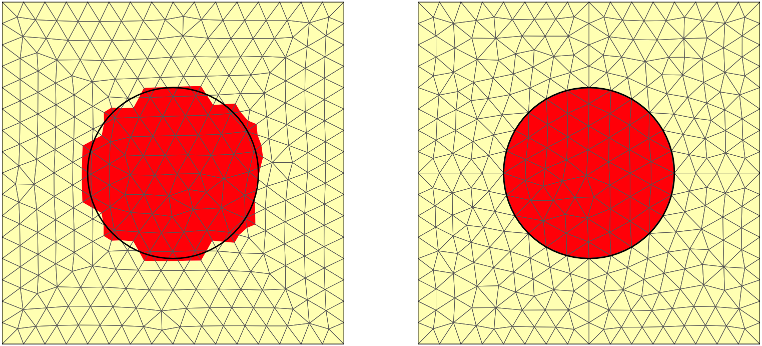

Laplace uniform capillary pressure $\boldsymbol{p_c = \sigma\,\kappa = \sigma/R = 400\,Pa}$ (whatever density) in a disk droplet of radius $\boldsymbol{R = 2.5\,10^{-3}\,m}$ for a constant surface tension $\boldsymbol{\sigma = 1\,N/m}$ (no gravity force, only the capillary force $\boldsymbol{f_c := \sigma\,\kappa\,\nabla\xi}$ on $\boldsymbol{\Sigma}$)

LEFT : Unstructured mesh non-fitted to the interface-markers circle

RIGHT : Unstructured mesh fitted to the interface $\boldsymbol{\Sigma}$

$\Rightarrow$ Null velocity field in both cases with no parasite current

2-D gas bubble rising in a liquid : dimensionless numbers
Hysing et al., IJNMF (2009) : two benchmark problems with different density/viscosity ratios and surface tension σ

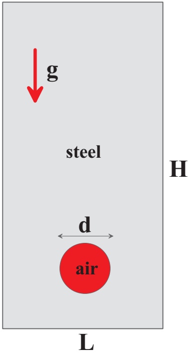

Air bubble initial diameter $\boldsymbol{d}$ in a vertical cavity $\boldsymbol{L \times H}$, $\boldsymbol{g = 9.81\, m/s^2}$
$\boldsymbol{\rho_l/\rho_g = 10}$ to $\boldsymbol{10^3}$, $\boldsymbol{\mu_l/\mu_g = 10}$ to $\boldsymbol{100}$, surface tension coefficient
$\boldsymbol{\sigma}_{\text{gas/liquid}} = \boldsymbol{0.07197\, N/m}$ (at $\boldsymbol{25\,^\circ C}$) to $\boldsymbol{2.50\, N/m}$ (large surface tension)
Characteristic gravitational velocity $\boldsymbol{U_g := \sqrt{g\, d}}$,
Reynolds number $\text{Re} := \boldsymbol{\rho_l\, U_g\, d/\mu_l}$, Eötvös number $\boldsymbol{Eo := \rho_l\, U_g^2\, d/\sigma}$

Standard benchmark for multiphase flows I

2-D dispersed two-phase bubble dynamics
Hysing et al., IJNMF (2009) : first benchmark pb with small density/viscosity ratios and surface tension
VPP_ε method with $\varepsilon = 10^{-8}$, mesh size=128×256, $\delta t = 0.007143$ and VOF-PLIC interface capturing

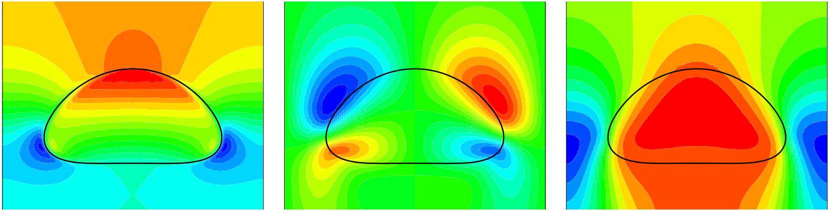

Motion of a circular bubble with surface tension at time $\boldsymbol{t = 3}$ - bubble initial diameter $\boldsymbol{d = 0.05\,m}$, $\boldsymbol{\rho_1/\rho_2 = 1000/100 = 10}$, $\boldsymbol{\mu_1/\mu_2 = 1/0.1 = 10}$, $\boldsymbol{\sigma = 2.45\,N/m}$, domain $\mathbf{0.1 \times 0.2}$, bubble initially circular with no motion at height $\boldsymbol{y = 0.05}$ – $\boldsymbol{g = 9.81\,m/s^2}$, ref. gravitational velocity $\boldsymbol{U_g := \sqrt{g\,d} = 0.700\,m/s}$, Reynolds number Re $\boldsymbol{:= \rho_1\,U_g\,d/\mu_1 = 35}$, Eötvös number $\boldsymbol{Eo := \rho_1\,U_g^2\,d/\sigma = 10}$
Left : isobars and isoline $\boldsymbol{\varphi = 0.5}$ of the phase fraction function at interface
Center : horizontal velocity field
Right : superposition of isoline $\boldsymbol{\varphi = 0.5}$ at interface for (UAL), (SIP), (VPP) and vertical velocity field (in absolute referential)

Sharp benchmark of two-phase bubble dynamics II

Air bubble rising in a liquid melted steel with VPP_ε or K-VPP_ε
PhA., Caltagirone and Fabrie, 4th T.I. Conf. (Hal, 2015)

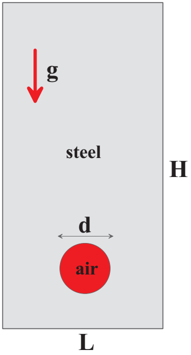

Air bubble initial diameter $d = 1\,cm$, $L = 4\,cm$, $H = 10\,cm$, $g = 9.81\,m/s^2$
$\rho_l/\rho_g \approx 8500$ or 10^4, $\mu_l/\mu_g \simeq 54$, $\sigma_{\text{air/steel}} = 1.50\,N/m$ (large surface tension)
$U_g := \sqrt{g\,d} = 0.313\,m/s$, Re $= 26\,632$, $Eo := \rho_1\,U_g^2\,d/\sigma = 5.55$
Isothermal computations at $\mathcal{T} = 800 - 900\,°C$ (melted steel) – $\varepsilon = 10^{-8}$
Symmetric/Non-symmetric flows with large shape deformations

Sharp benchmark of two-phase bubble dynamics II

K-VPP$_\varepsilon$ with $\varepsilon = 10^{-10}$, mesh size=128×256, $N = 128$
Lagrangian front tracking markers, δt such that $CFL = 0.5$

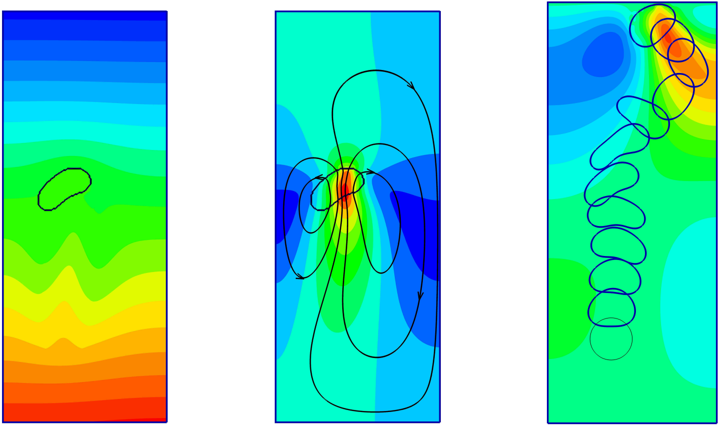

LEFT : pressure field $\boldsymbol{p} \in [\mathbf{-9235,\ 0}]\ \boldsymbol{Pa}$ ($\boldsymbol{p} = \mathbf{0}$ at bottom left) at time $\boldsymbol{t} = \mathbf{0.05}\ \boldsymbol{s}$
CENTER : vertical velocity field $\boldsymbol{v_z} \in [\mathbf{-0.48,\ 1.55}]\ \boldsymbol{m/s}$ and streamlines at $\boldsymbol{t} = \mathbf{0.05}\ \boldsymbol{s}$ – RIGHT : Some bubble positions and shapes during time and vertical velocity field $\boldsymbol{v_z}$ at final time $\boldsymbol{t} = \mathbf{0.2}\ \boldsymbol{s}$.

Outlines

Vector penalty-projection methods for low-Mach variable density and multiphase flows or fluid-structure interaction

- $\Rightarrow$ Methods VPP$_\varepsilon$/K-VPP$_\varepsilon$ efficient to solve Darcy and Navier-Stokes/Brinkman problems :
  - whatever density, viscosity or anisotropic permeability jumps
  - under strong stresses : large surface tension and shape deformation
  - with Dirichlet or Neumann stress boundary conditions
- $\Rightarrow$ Design with **4** key ideas or features :
  - Fully vector-consistent formulation for primary unknowns $(\boldsymbol{v}, \boldsymbol{\nabla p})$:
    $\Rightarrow$ accurate and curl-free component $\widehat{\boldsymbol{v}}^{n+1} := \boldsymbol{v}^{n+1} - \widetilde{\boldsymbol{v}}^{n+1}$ of $\widetilde{\boldsymbol{v}}^{n+1}$
    $\Rightarrow$ get rid of scalar pressure Poisson equation and its spurious B.C.
  - New fast Helmholtz-Hodge decompositions of $\mathbf{L^2}$-vector fields :
    $\Rightarrow$ splitting penalty method for saddle-point with adapted r.h.s.
  - VPP$_\varepsilon$: mass density $\boldsymbol{\rho}$ only included in the diagonal term :
    $\Rightarrow$ cheap diagonal preconditioning for variable density
  - K-VPP$_\varepsilon$: kinematic VPP completely independent of $\boldsymbol{\rho}$ on edge-based MAC mesh :
    $\Rightarrow$ Robustness : insensitive to large variations of density $\boldsymbol{\rho}$
- $\Rightarrow$ Accurate, Fast and Robust methods

Conclusion

See my Google Scholar profile for the preprints

- Second-order accuracy in time with BDF2 or Crank-Nicolson schemes : Ok
- Open (Neumann stress) boundary conditions : Ok
- Optimal error estimates for Navier-Stokes problems with Dirichlet or Neumann B.C. : Ok

- $\mathrm{VPP}_{\varepsilon}/\mathrm{K\text{-}VPP}_{\varepsilon}$ methods for low Mach number flows now the parameter ε must be chosen such that :

$$\varepsilon\,\delta t = \chi_{\mathcal{T}} = \gamma\,\chi_S = \frac{\gamma\,\mathrm{M}^2}{\rho\,V^2} \quad \text{or} \quad \gamma\,\mathrm{M}^2 = \rho\,V^2\,(\varepsilon\,\delta t) \ll 1$$

  where
  - $\chi_{\mathcal{T}}, \chi_S$: isothermal or isentropic compressibility coefficients of the fluid
  - $\gamma := c_p/c_v \geq 1$, *i.e.* ratio of heat capacities of the fluid
  - Mach number : $\mathrm{M} := V/c$
  - V : given reference velocity
  - c : speed of acoustic waves in the fluid

Some perspectives...

- Other preconditioner than IC/ILU : SSOR, Multigrid, DDM ...
- Parallel efficiency, scalability ...

- Theoretical analysis for homogeneous Navier-Stokes :
  unconditional stability, convergence, error estimates
  $\Rightarrow$ Ok for both Dirichlet and open boundary conditions
- Theoretical analysis for non-homogeneous multiphase Navier-Stokes :
  open problem without regularization : Ok for K-VPP$_{\varepsilon}$

- Magnetohydrodynamics (MHD) or plasma transport problems :
  $\Rightarrow \operatorname{div} \boldsymbol{B} = \mathbf{0}$
- fluid-structure interaction problems with Discrete Mechanics :
  Caltagirone and PhA., Turbulence & Interactions Conf. (2018)
  in Proceedings book, Springer (2021)

Thank you for attention